Published in final edited form as:
Nature. 2011 April 14; 472(7342): 230–233. doi:10.1038/nature09932.

Structure of Mammalian AMPK and its regulation by ADP

Bing Xiao[1,3], **Matthew J. Sanders**[2,3], **Elizabeth Underwood**[1,3], **Richard Heath**[1,3], **Faith Mayer**[2], **David Carmena**[2], **Chun Jing**[1], **Philip A. Walker**[1], **John F. Eccleston**[1], **Lesley F. Haire**[1], **Peter Saiu**[1], **Steven A. Howell**[1], **Rein Aasland**[1], **Stephen R. Martin**[1], **David Carling**[2], and **Steven J. Gamblin**[1]

[1] MRC National Institute for Medical Research, The Ridgeway, Mill Hill, London NW7 1AA, UK

[2] MRC Clinical Sciences Centre, Hammersmith Hospital Campus, Imperial College, DuCane Road, London W12 0NN, UK

Abstract

The heterotrimeric AMP-activated protein kinase (AMPK) plays a key role in regulating cellular energy metabolism; in response to a fall in intracellular ATP levels it activates energy producing pathways and inhibits energy consuming processes[1]. AMPK has been implicated in a number of diseases related to energy metabolism including type 2 diabetes, obesity and, most recently, cancer [2,3,4,5,6]. AMPK is converted from an inactive to catalytically competent form by phosphorylation of the activation loop within the kinase domain[7]; AMP binding to the γ regulatory domain promotes phosphorylation by the upstream kinase[8], protects the enzyme against dephosphorylation as well as causing allosteric activation[9]. We show here that ADP binding to just one of the two exchangeable AXP binding sites on the regulatory domain protects the enzyme from dephosphorylation, although it does not lead to allosteric activation. Our studies show that active AMPK displays significantly tighter binding to ADP than to Mg.ATP, explaining how the enzyme is regulated under physiological conditions where the concentration of Mg.ATP is higher than that of ADP and much higher than that of AMP. We have determined the crystal structure of an active AMPK complex. It shows how the activation loop of the kinase domain is stabilized by the regulatory domain and how the kinase linker region interacts with the regulatory nucleotide binding site that mediates protection against dephosphorylation. From our biochemical and structural data we develop a model for how the energy status of a cell regulates AMPK activity (Supplementary Fig. 1).

At the whole body level, AMPK is regulated by a diverse range of hormones e.g. leptin[10], adiponectin[11], ciliary neurotrophic factor[12] and ghrelin[13] and it plays a role in appetite[13,14], glucose, lipid and protein metabolism[1,3,15], cell growth and cell polarity [2,4]. AMPK is a heterotrimeric complex comprising an α catalytic subunit and two regulatory subunits (β and γ)[1]. Activation of AMPK requires phosphorylation of Thr-172 which lies in the activation segment of the N-terminal kinase domain of the α subunit[7]. Phosphorylation of Thr-172 leads to a several hundred fold increase in activity[9,16]. In mammals, calcium/calmodulin-dependent protein kinase kinase β (CaMKKβ) and LKB1 are the predominant kinases upstream of AMPK, although there is some evidence implicating other upstream kinases [17,18]. Previous studies have shown that AMP protects against the dephosphorylation

Correspondence and requests for materials should be addressed to D.C. (david.carling@csc.mrc.ac.uk) or S.J.G. (sgambli@nimr.mrc.ac.uk)..

[3]These authors contributed equally to this work

Author Contributions B.X., M.J.S., E.U., R.H., F.M., D.J.C., C.J., P.A.W., J.F.E., L.F.H., P.S., S.A.H., R.A. & S.R.M. performed experiments. All authors contributed to data analysis, experimental design and manuscript writing.

Coordinates have been deposited in the Protein Data Bank with accession codes 1XYZ, 2XYZ, 3XYZ and 4XYZ.

Europe PMC Funders Author Manuscripts

of Thr-172[16],[19] and we recently provided evidence that protection against dephosphorylation is the major physiological mechanism for activation of AMPK[9]. In addition to activation by phosphorylation, AMP causes a 2-5 fold allosteric activation of AMPK depending on the nature of the isoforms present in the AMPK complex[20]. To address this issue we previously investigated the nucleotide binding properties of the γ1 subunit of AMPK and determined the structure of the regulatory core of mammalian AMPK (α C-terminal domain, β C-terminal domain, full-length γ domain; hereafter referred to as the regulatory fragment) in complex with nucleotides[21]. Importantly, our studies revealed that three of the four potential nucleotide binding sites are occupied[21]. One of these sites contains a permanently bound AMP molecule (site-4 based on the nomenclature suggested by Kemp *et al.*[22]), whereas AMP and Mg.ATP compete for binding at the other two sites[21] (site-1 and site-3).

Unlike AMP, ADP has no significant allosteric effect on AMPK isolated from rat liver[23]. Consistent with this, we also find that ADP does not activate recombinant AMPK under conditions where AMP produces a 2-fold activation (Fig. 1a). Importantly however, our studies show that ADP provides protection of AMPK from dephosphorylation across a similar range of concentrations as AMP (Fig. 1b). We have also shown the same effect using AMPK purified from rat liver (Supplementary Fig. 2a). While Mg.ATP does not protect against dephosphorylation (Fig. 1c), it does compete with the protective effect of both AMP and ADP on dephosphorylation (Fig. 1d). We have also shown that the protective effect of ADP is lost in a Wolff-Parkinson-White syndrome mutation (Supplementary Fig. 2b). We envisage that AMP/ADP binding shifts the equilibrium between dephosphorylation sensitive and insensitive states, and thus slows, but does not abolish, dephosphorylation of the enzyme by phosphatases.

Extending our earlier work looking at nucleotide binding to the regulatory fragment, we characterized binding of nucleotides to active full-length AMPK. For these studies we used CaMKKβ to stoichiometrically phosphorylate Thr-172 on the activation loop of recombinant full-length AMPK and used the coumarin adducts of ATP and ADP as fluorescent reporters of nucleotide binding and derived the binding parameters for the unlabeled nucleotides by competition experiments (Fig. 2a). We verified that the two species bind at the same sites by determining the crystal structures of the regulatory fragment in complex with coumarin-ADP and with ADP (Supplementary Fig. 3). The results show (Table 1) that the two exchangeable sites have markedly different affinities for nucleotides. Binding at the tighter of the two sites is at least 30-fold stronger than at the weaker site. Given that under physiological conditions, most of the ATP is coordinated to Mg^{2+}, and the majority of AMP and ADP is not, we also measured nucleotide binding in the presence of this cation. The data show that Mg.ATP binds up to 10-fold weaker than ATP. Thus, active AMPK binds AMP/ADP significantly more strongly than it does Mg.ATP at both exchangeable sites. There are two lines of evidence that lead us to conclude that it is AMP/ADP binding at the weaker of the two exchangeable sites that accounts for the protection of the enzyme against dephosphorylation. The first is that the dose response curve for AMP/ADP mediated protection against phosphorylation correlates with the binding curves for these nucleotides at the weaker, rather than the stronger, of the two binding sites (Fig. 1b). The second comes from our discovery that NADH binds to AMPK.

NADH undergoes a significant change in fluorescence upon binding to AMPK. We used this property to establish that the cofactor binds to a single site on the enzyme, with a dissociation constant of about 50 μM (Fig. 2b - inset). NADH binding is competed by AXPs binding to the stronger, but not the weaker, of the two exchangeable sites (Fig. 2b & Table 1). When we repeated the ADP protection against dephosphorylation experiments using a range of NADH concentrations, we found no evidence for NADH competing with the

protective effect of ADP on dephosphorylation whereas NADH, and ADP, both compete with AMP for allosteric activation of the enzyme (Supplementary Fig 4). This observation argues that it is AMP/ADP binding at the weaker of the two exchangeable sites, the one that does not bind NADH, which is responsible for protection against dephosphorylation. We also carried out co-crystallization of the regulatory fragment with one molar equivalent of ADP (Supplementary Fig. 5). The resulting electron density map showed full occupancy of ADP at site-1 and no detectable density at site-3, identifying site-3 as the weaker binding site. We can therefore assign the allosteric effect to AMP binding at the tighter site-1 and protection against dephosphorylation is mediated by AMP/ADP binding at the weaker site-3.

Previous studies on the regulation of AMPK have focused on the role of AMP because it allosterically activates the enzyme[15] while ADP does not. However, phosphorylation remains central to AMPK regulation since the enzyme is inactive in the absence of Thr-172 phosphorylation[7,16]. Under optimal conditions, mammalian cells maintain ATP at a high level relative to ADP and AMP. Typical concentrations of free adenine nucleotides in mammalian cells lie in the range of 3000-8000 μM for ATP, 50-200 μM for ADP and 0.5-5 μM for AMP[24,25,26]. Since the free concentration of ADP is between 10 to 400-fold higher than AMP, and their binding constants are similar, ADP will be more successful at competing with Mg.ATP than AMP. Therefore, the fact that ADP protects AMPK from dephosphorylation is likely to represent an important physiological mechanism for regulating the activity of the enzyme.

We have also determined the crystal structure of an active form of the enzyme that encompasses the whole of the catalytic α subunit. The construct used is shown in Figure 3a (details of its design are given in Supplementary Fig. 6). From the best samples we collected a dataset to 3.3 Å Bragg spacing, after screening about 100 crystals, and solved the structure by molecular replacement using independent models for the regulatory fragment (2V8Q)[21] and the kinase domain (2H6D)[27]. Although the dataset is at medium resolution, the molecular replacement solution was robust and yielded initial electron density which revealed the location of many components that were not present in the original model. As might be expected for a structure of this complexity and resolution, some parts of the molecule are better defined than others. For example, the activation loop of the kinase domain, which is packed against the regulatory fragment, has better defined electron density than loops on the surface of the complex which often show continuous main-chain density but lack side chain features. Overall, the most important features of the current structure concern the architecture of the complex, particularly the relationships between the α–kinase domain and the α-linker with the regulatory fragment (omit maps for these regions are presented in Supplementary Fig. 7).

The structure is shown in Ribbons representation (Fig. 3b,c, Supplementary Fig. 8) and in space filling representation before, and after, the kinase domain and the linker region have been rotated away from the complex to display their contact regions (Fig. 3d). The first of these interfaces involves the kinase domain and has a surface area of about 1100 $Å^2$. This relatively modest contact area is consistent with the observation that specific protease cleavage of the linker between the kinase domain and the C-terminal domain of the α subunit leads to material that separates into two components (kinase domain + regulatory fragment) following gel filtration. A significant part of the contact area involves the activation loop of the kinase interacting predominantly with the C-terminus of the β domain (Fig 3c). Unlike previous structures of the isolated, and non-phosphorylated kinase domain, the phosphorylated activation loop in our structure is well ordered, as evidenced by electron density maps (Supplementary Fig. 7). The small lobe of the kinase is in a more closed conformation relative to the unphosphorylated (and thus inactive) isolated kinase domain

structure[27] (Supplementary Fig. 9). The fact that the activation loop mediates the interaction of the kinase domain with the regulatory fragment means that, in this conformation, Thr-172 is protected from access by phosphatases. This idea is strongly supported by site-directed mutagenesis experiments; mutation of β1 His-233 (corresponding to His-235 in β2), at the interface with the kinase domain (Fig. 3c), results in an enzyme which is activatable by phosphorylation but which has a significantly increased rate of dephosphorylation in phosphatase assays (Fig. 4a, b).

Another component of the α subunit/regulatory interaction is provided by a part of the segment of the α chain which links the N-terminal kinase domain to the C-terminal regulatory fragment, involving residues between α373 and α382 that are largely conserved between α1 and α2 in vertebrates (Supplementary Fig. 10) which we have called the α-hook structure (Fig. 3b, d). The α-hook interacts with the γ subunit at the exchangeable binding site-3, with AMP bound, that we have assigned as the weaker of the two sites that is responsible for mediating AMP/ADP protection against dephosphorylation. The hook makes a lid over the nucleotide binding site that accounts for a buried surface area of about 500 Å^2. We obtained crystals of this construct with AMP added to the crystallization mixture and an AMP molecule is clearly identifiable in the electron density maps at site-3, as well as at the non-exchangeable site. Although we did not see AMP at site-1 in the initial crystals, we subsequently achieved good occupancy at this site by maintaining a higher concentration of AMP during crystallization and handling procedures (data not shown). In contrast we think that the AMP at site-3 is held in place by the arrangement of the α-hook and that it would have to dissociate before the bound AMP could be released and then exchanged. Based on superposition of our earlier structures of the regulatory fragment of AMPK in complex with ADP and Mg.ATP and the structure presented here, we think that the α-hook sequence cannot interact with site-3 when Mg.ATP is bound mainly due to the change in conformation of γ Arg-69 which would generate a steric clash with the hook (Supplementary Fig. 11). To test the role of the α-hook in mediating protection against dephosphorylation we generated a mutant in this region (R375Q/T377A/D379A/E380A). The resulting enzyme was allosterically activated by AMP but was not subject to protection against dephosphorylation by AMP or ADP (Fig. 4c, d). Interestingly, the mutation at His-233 described above does retain some protective effect of AMP/ADP (Fig. 4a, b). Given that this mutation would be expected to weaken the interaction between the kinase domain and the regulatory fragment, but not block it, it seems reasonable that AMP/ADP binding would still help to order the α-hook and thus facilitate the recruitment of the kinase domain.

Taking our biochemical and structural data together, we propose the following model for how AMP/ADP, but not Mg.ATP, protects AMPK against dephosphorylation, and thus inactivation (Supplementary Fig. 1). We have demonstrated that the protective effect of AMP/ADP is mediated by its binding to the weaker of the two exchangeable sites which we have identified as site-3. We have also shown that the α-hook region binds into this site in the presence of AMP and predict that the same situation would occur with ADP. We further suggest that binding of the α-hook acts to restrict the flexibility of the preceding α linker region (residues 300 to 370) and, in so doing, promotes the interaction of the kinase domain with the regulatory fragment seen in our crystal structure. This interaction, which mostly involves contacts between the activation loop and the C-terminal domain of β, would therefore act to protect Thr-172 against dephosphorylation. Since the interaction surface of the α–hook with the regulatory fragment is relatively small it is likely that there is a dynamic equilibrium between the α–hook bound and α–hook unbound species. If, as our structure suggests, AMP/ADP binding favours the α–hook bound species but Mg.ATP binding drives formation of the α–hook unbound species, then the competitive binding of AMP/ADP versus Mg.ATP would control the extent to which the enzyme was protected from dephosphorylation and inactivation.

Methods Summary

AMPK complexes were expressed in *E. coli* BL21 (DE3) cells, purified by affinity chromatography using nickel-Sepharose and phosphorylated by incubation with CaMKKβ as described previously[9]. AMPK activity was determined using 0.2 mM SAMS peptide[9], 0.2 mM ATP and 5 mM $MgCl_2$. Dephosphorylation of AMPK by recombinant PP2Cα was monitored either by measuring AMPK activity using the SAMS peptide assay or by Western blotting of phospho-T172. Western blot signals for phospho-T172 and total AMPK α subunit (determined using sheep anti-α1 or anti-α2 antibodies) were quantified using the Li-Cor Odyssey infrared imaging system. Uncorrected fluorescence spectra of the nucleotides (3′-(7-diethylaminocoumarin-3-carbonylamino)-3′-deoxy-ADP (C-ADP), and 3′-(7-diethylaminocoumarin-3 carbonylamino)-3′-deoxy-ATP (C-ATP) (both generous gifts from Dr. Martin Webb, MRC NIMR, London)) and NADH and their complexes were recorded at 20°C using a Jasco FP-6300 fluorimeter. Binding of nucleotides was monitored by titrating nucleotide (4-10 μM) with AMPK. Dissociation constants for AMP, ADP, and ATP were determined using competition assays. The engineered crystallization construct was expressed as a His-tag fusion protein in *E. coli*. Purified protein was phosphorylated using CAMKKβ before mixing with AMP and staurosporine. Crystals were grown by the hanging drop method using isopropanol and MPD as precipitant. Diffraction data were collected on the Diamond Light Source, Oxford and processed using Denzo and Scalepack[28]. The structure was solved by molecular replacement using Amore[29] and standard refinement was carried out with Refmac5[30] with manual model building with COOT. Figures were created with Pymol (http://pymol.sourceforge.net/).

Supplementary Material

Refer to Web version on PubMed Central for supplementary material.

Acknowledgments

We thank Martin Webb for gift of coumarin nucleotides and John Skehel for comments on the manuscript and Stephen Smerdon for discussion and assistance. Work in both laboratories is supported by the MRC and we gratefully acknowledge Diamond Light Source for synchrotron access.

References

1. Carling D. The AMP-activated protein kinase cascade--a unifying system for energy control. Trends Biochem Sci. 2004; 29:18–24. [PubMed: 14729328]
2. Hardie DG. AMP-activated/SNF1 protein kinases: conserved guardians of cellular energy. Nat Rev Mol Cell Biol. 2007; 8:774–785. [PubMed: 17712357]
3. Kahn BB, Alquier T, Carling D, Hardie DG. AMP-activated protein kinase: ancient energy gauge provides clues to modern understanding of metabolism. Cell Metab. 2005; 1:15–25. [PubMed: 16054041]
4. Shackelford DB, Shaw RJ. The LKB1-AMPK pathway: metabolism and growth control in tumour suppression. Nat Rev Cancer. 2009; 9:563–575. [PubMed: 19629071]
5. Cool B, et al. Identification and characterization of a small molecule AMPK activator that treats key components of type 2 diabetes and the metabolic syndrome. Cell Metab. 2006; 3:403–416. [PubMed: 16753576]
6. Huang X, et al. Important role of the LKB1-AMPK pathway in suppressing tumorigenesis in PTEN-deficient mice. Biochem J. 2008; 412:211–221. [PubMed: 18387000]
7. Stein SC, Woods A, Jones NA, Davison MD, Carling D. The regulation of AMP-activated protein kinase by phosphorylation. Biochem J. 2000; 345(Pt 3):437–443. [PubMed: 10642499]

8. Oakhill JS, et al. beta-Subunit myristoylation is the gatekeeper for initiating metabolic stress sensing by AMP-activated protein kinase (AMPK). Proc Natl Acad Sci U S A. 2010; 107:19237–19241. [PubMed: 20974912]
9. Sanders MJ, Grondin PO, Hegarty BD, Snowden MA, Carling D. Investigating the mechanism for AMP activation of the AMP-activated protein kinase cascade. Biochem J. 2007; 403:139–148. [PubMed: 17147517]
10. Minokoshi Y, et al. Leptin stimulates fatty-acid oxidation by activating AMP-activated protein kinase. Nature. 2002; 415:339–343. [PubMed: 11797013]
11. Yamauchi T, et al. Adiponectin stimulates glucose utilization and fatty-acid oxidation by activating AMP-activated protein kinase. Nat Med. 2002; 8:1288–1295. [PubMed: 12368907]
12. Watt MJ, et al. CNTF reverses obesity-induced insulin resistance by activating skeletal muscle AMPK. Nat Med. 2006; 12:541–548. [PubMed: 16604088]
13. Andersson U, et al. AMP-activated protein kinase plays a role in the control of food intake. J Biol Chem. 2004; 279:12005–12008. [PubMed: 14742438]
14. Minokoshi Y, et al. AMP-kinase regulates food intake by responding to hormonal and nutrient signals in the hypothalamus. Nature. 2004; 428:569–574. [PubMed: 15058305]
15. Hardie DG, Carling D, Sim ATR. The AMP-activated protein kinase: a multisubstrate regulator of lipid metabolism. Trends Biochem Sci. 1989; 14:20–23.
16. Suter M, et al. Dissecting the role of 5′-AMP for allosteric stimulation, activation, and deactivation of AMP-activated protein kinase. J Biol Chem. 2006; 281:32207–32216. [PubMed: 16943194]
17. Carling D, Sanders MJ, Woods A. The regulation of AMP-activated protein kinase by upstream kinases. Int J Obes (Lond). 2008; 32(Suppl 4):S55–59. [PubMed: 18719600]
18. Momcilovic M, Hong SP, Carlson M. Mammalian TAK1 activates Snf1 protein kinase in yeast and phosphorylates AMP-activated protein kinase in vitro. J Biol Chem. 2006; 281:25336–25343. [PubMed: 16835226]
19. Davies SP, Helps NR, Cohen PT, Hardie DG. 5′-AMP inhibits dephosphorylation, as well as promoting phosphorylation, of the AMP-activated protein kinase. Studies using bacterially expressed human protein phosphatase-2C alpha and native bovine protein phosphatase-2AC. FEBS Lett. 1995; 377:421–425. [PubMed: 8549768]
20. Cheung PC, Salt IP, Davies SP, Hardie DG, Carling D. Characterization of AMP-activated protein kinase gamma-subunit isoforms and their role in AMP binding. Biochem J. 2000; 346(Pt 3):659–669. [PubMed: 10698692]
21. Xiao B, et al. Structural basis for AMP binding to mammalian AMP-activated protein kinase. Nature. 2007; 449:496–500. [PubMed: 17851531]
22. Kemp BE, Oakhill JS, Scott JW. AMPK structure and regulation from three angles. Structure. 2007; 15:1161–1163. [PubMed: 17937905]
23. Carling D, Clarke PR, Zammit VA, Hardie DG. Purification and characterization of the AMP-activated protein kinase. Copurification of acetyl-CoA carboxylase kinase and 3-hydroxy-3-methylglutaryl-CoA reductase kinase activities. Eur J Biochem. 1989; 186:129–136. [PubMed: 2598924]
24. Veech RL, Lawson JW, Cornell NW, Krebs HA. Cytosolic phosphorylation potential. J Biol Chem. 1979; 254:6538–6547. [PubMed: 36399]
25. Hellsten Y, Richter EA, Kiens B, Bangsbo J. AMP deamination and purine exchange in human skeletal muscle during and after intense exercise. J Physiol. 1999; 520(Pt 3):909–920. doi:PHY_9256 [pii]. [PubMed: 10545153]
26. McConell GK, et al. Short-term exercise training in humans reduces AMPK signalling during prolonged exercise independent of muscle glycogen. J Physiol. 2005; 568:665–676. [PubMed: 16051629]
27. Littler DR, et al. A conserved mechanism of autoinhibition for the AMPK kinase domain: ATP-binding site and catalytic loop refolding as a means of regulation. Acta Crystallogr Sect F Struct Biol Cryst Commun. 2010; 66:143–151.
28. Otwinowski, Z.; Minor, W. Proceedings of the CCP4 Study Weekend. SERC Daresbury Laboratory; Warrington: 1993. Data Collection and Processing; p. 556-562.1993

29. Navaza J. AMoRe: an Automated Package for Molecular Replacement. Acta Crystallogr A. 1994; 50:157–163.
30. CCP4. The CCP4 suite: programs for protein crystallography. Acta Crystallogr D. 1994; 50:760–763. [PubMed: 15299374]

Europe PMC Funders Author Manuscripts

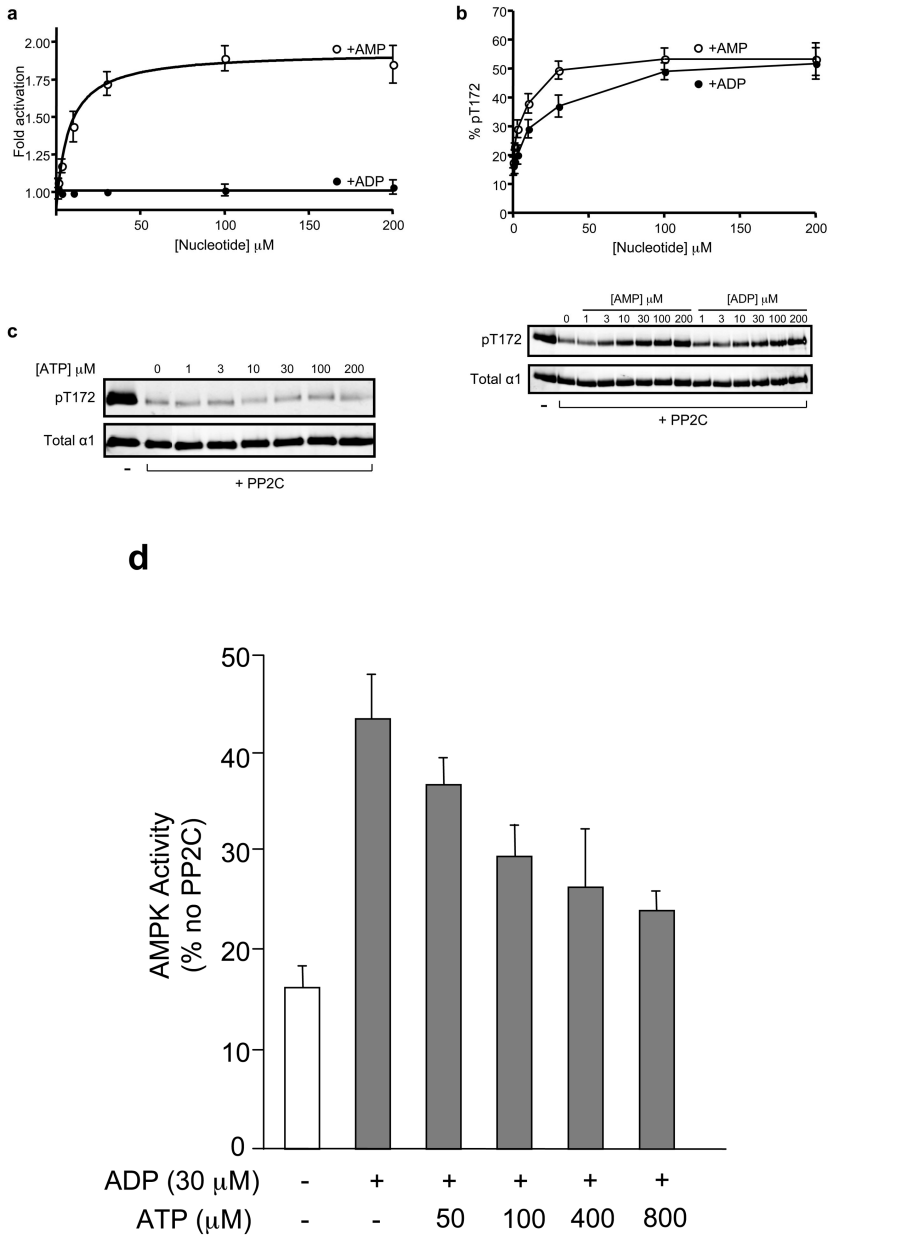

Figure 1. Role of ADP in regulation of AMPK activity

(a) AMP, but not ADP, allosterically activates AMPK. **(b)** AMP and ADP protection of AMPK from dephosphorylation. **(c)** ATP does not protect against dephosphorylation. **(d)** Mg.ATP competes with the protective effect of ADP on dephosphorylation. Results are displayed as the mean ± S.E.M determined from at least 3 independent experiments. Where appropriate a representative blot (n=3) showing Thr-172 phosphorylation and total α subunit levels is shown.

Europe PMC Funders Author Manuscripts

Europe PMC Funders Author Manuscripts

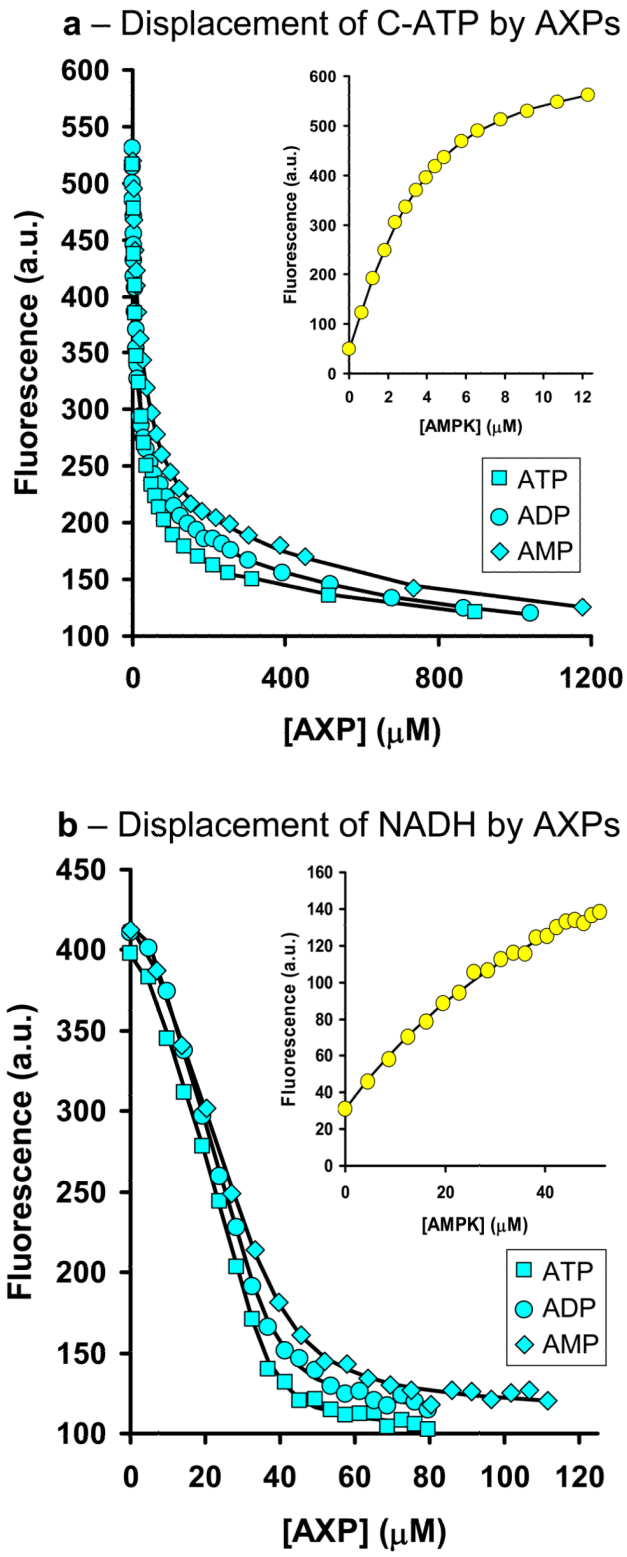

Figure 2. Measurement of equilibrium dissociation constants for the binding of AXPs to phosphorylated AMPK

(a) Displacement of Coumarin-ATP from the AMPK:(Coumarin-ATP)$_2$ complex by AXPs monitored using fluorescence at 470 nm. Solid lines are the computed best fits with $K_{d,I}$ and $K_{d,II}$ for C-ATP binding to AMPK fixed at 1.1 and 4.2 μM. Inset: Titration of Coumarin-ATP with AMPK. **(b)** Displacement of NADH from the AMPK:NADH complex by AXPs monitored using fluorescence at 435 nm. The solid line is the computed best fit with the K_d for NADH fixed at 65 μM. Inset: Fluorescence titration of NADH with AMPK.

Europe PMC Funders Author Manuscripts

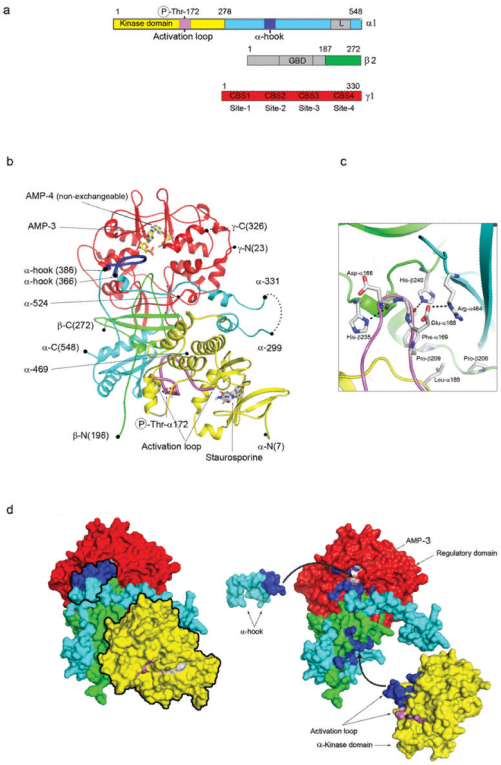

Figure 3. Crystal structure of active mammalian AMPK

(a) Schematic representation of the components of the heterotrimer; the parts of the complex missing from the crystallized protein are shown in grey. The domains, including the activation loop (pink) and α-hook (dark blue), are coloured the same in all panels. **(b)** Ribbon representation of the crystallized complex with two the bound AMPs, staurosporine and phospho Thr-172 shown in stick representation. The α-hook and activation loop of the kinase domain are shown in heavier lines and coloured dark blue and pink respectively. **(c)** The interface between the activation loop and the regulatory fragment are shown in more detail in a similar orientation as (b), potential electrostatic interactions are indicated by dashed lines. **(d)** The complex is shown in two space-filling representations. The left panel represents the same view as (b) with the α-hook and kinase domain outlined in black. In the right hand panel these two components have been rotated away from the regulatory domain to show the interaction surfaces in an 'open-book' representation, where the contacting residues have been coloured in dark blue. With the α-hook removed, AMP-3 becomes visible. The black arrows indicate the rotations that would reassemble the complex.

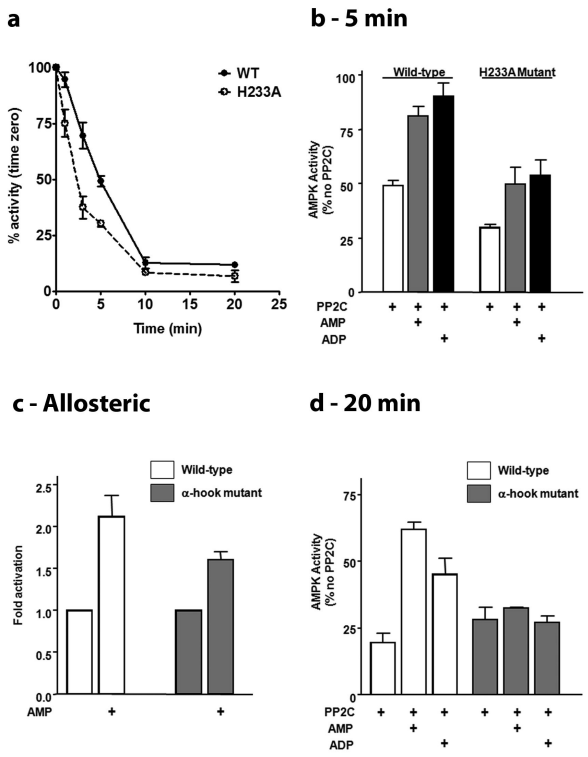

Figure 4. Mutational analysis of AMPK regulation

(a) Desphophorylation rate of the wild-type (WT) or β His-233 to alanine kinase domain interface mutant (H233A, corresponding to H235A in β2). **(b)** Protection of dephosphorylation of WT or H233A mutant by AMP (30 μM) or ADP (30 μM) after incubation for 5 mins. **(c)** Allosteric activation of WT or α-hook mutant (harbouring mutation of residues R375Q, T377A, D379A and E380A within α1) by AMP (100 μM). **(d)** AMP (30 μM) and ADP (30 μM) protection of WT or α-hook mutant from dephosphorylation. Results are the mean ± S.E.M from at least 3 independent experiments

Europe PMC Funders Author Manuscripts

Europe PMC Funders Author Manuscripts

Table 1

Equilibrium dissociation constants for the binding of AXPs to phosphorylated AMPK.

Ligand	K_d (μM)	$K_{d,I}$ (μM)	$K_{d,II}$ (μM)
	vs NADH	*vs* C-AXPs	
AMP	1.6 (0.5)	2.5 (0.6)	80 (25)
ADP	1.3 (0.5)	1.5 (0.4)	50 (15)
ATP	0.9 (0.3)	1.7 (0.5)	65 (15)
Mg-ATP	32 (12)	18 (7.5)	230 (80)

Dissociation constants were determined at 20°C by competition against NADH or C-AXPs in 25 mM Tris, 1 mM TCEP, 100 mM NaCl (pH 8) with and without 5 mM MgCl2. The K_d values are reported as the mean (± SD) determined from at least three independent measurements.